Pile-Driving Analysis by One-Dimensional Wave Theory: State of the Art

T. J. HIRSCH, L. L. LOWERY, H. M. COYLE, and C. H. SAMSON, JR.,
College of Engineering, Texas A&M University

The numerical computer solution of the one-dimensional wave equation can be used with reasonable confidence for the analysis of pile-driving problems. The wave equation can be used to predict impact stresses in a pile during driving and to estimate the static soil resistance on a pile at the time of driving from driving records. If this method of analysis is used, the effects of significant parameters can be evaluated during the foundation design stage. These parameters include type and size of pile-driving hammer; driving assemblies such as cap block, helmet, and cushion block; type and size of pile; and soil condition. From such an analysis appropriate piles and driving equipment can be selected to correct or avoid expensive and time-consuming construction problems, such as excessive driving stresses or pile breakage and inadequate equipment, to achieve desired penetration or bearing capacity. Wave-equation evaluation of data from the Michigan pile study indicated that a relatively simple formula can be used to determine the energy output for both steam and diesel pile-driving hammers.

To date, the wave equation has been compared with the results of 43 actual field tests performed throughout the country, and the results are encouraging. The driving accessories significantly affect the piling behavior, and, therefore, their selection should be carefully considered and analyzed whenever possible. The effect of pile dimensions on ability to drive the pile varied greatly; generally, stiffer piles can overcome greater soil resistance to penetration. The wave equation can be used to estimate soil resistance on a pile at the time of driving. Before long-term bearing capacity can be extrapolated from this resistance, however, engineers must consider the effect of soil setup or relaxation, and other time effects that might be important.

•THE TREMENDOUS INCREASE in the use of piles in both landbased and offshore foundation structures and the appearance of new pile-driving methods have created great engineering interest in finding more reliable methods for the analysis and design of piles. Since Isaacs' paper (1), it has been recognized that the behavior of piling during driving does not follow the simple Newtonian impact as assumed by many simplified pile-driving formulas but rather is governed by the one-dimensional wave equation. Unfortunately, an exact mathematical solution to the wave equation was not possible for most practical pile-driving problems.

In 1950, Smith (2) developed a tractable solution to the wave equation that could be used to solve extremely complex pile-driving problems. The solution was based on a discrete element idealization of the actual hammer-pile-soil system coupled with the use of a high-speed digital computer. In a paper published in 1960 (3), he dealt exclusively with the application of wave theory to the investigation of the dynamic behavior of piling during driving.

Paper sponsored by Committee on Substructures, Retaining Walls and Foundations and presented at the 49th Annual Meeting.

SOLUTION TO THE WAVE EQUATION

Smith's Numerical Solution

This solution is based on dividing the distributed mass of the pile into a number of concentrated weights, W(1) through W(p), which are connected by weightless springs, K(1) through K(p - 1), and adding soil resistance that acts on the masses, as shown in Figure 1. Time is also divided into small increments. For the idealized system, Smith set up a series of equations of motion in the form of finite difference equations that were easily solved by using high-speed digital computers. He extended his original method of analysis to include various nonlinear parameters such as elastoplastic soil resistance including velocity damping and others.

Figure 1 shows the idealization of the pile system suggested by Smith. In general, the system is considered to be composed of the following:

1. A ram, to which an initial velocity is imparted by the pile driver;
2. A cap block (cushioning material);
3. A pile cap;
4. A cushion block (cushioning material);
5. A pile; and
6. The supporting medium, or soil.

In Figure 1 the ram, cap block, pile cap, cushion block, and pile are shown as appropriate discrete weights and springs. The frictional soil resistance on the side of the pile is represented by a series of side springs; the point resistance is accounted for by a single spring at the point of the pile. The characteristics of these various components will be discussed in greater detail later in this report.

Actual situations may deviate from the one shown in Figure 1. For example, a cushion block may not be used or an anvil may be placed between the ram and cap block. However, such cases are readily accommodated.

External Springs—The resistance to dynamic loading afforded by the soil in shear along the outer surface of the pile and in bearing at the point of the pile is extremely complex. Figure 2 shows the load-deformation characteristics that Smith assumed the soil to have, exclusive of damping effects. The path OABC DEFG represents loading and unloading in side friction. For the point, only compressive loading may take place and the loading and unloading path would be along OABCF.

The characteristics shown in Figure 2 are defined essentially by the quantities

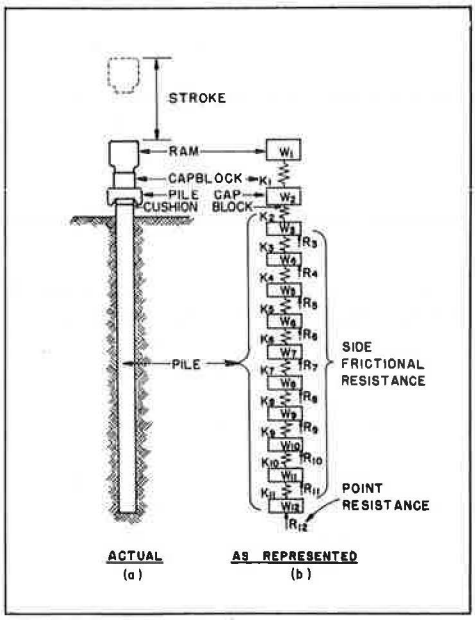

Figure 1. Method of representing pile for purpose of analysis (after Smith).

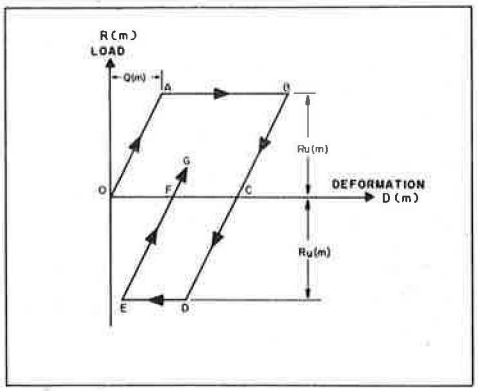

Figure 2. Load-deformation characteristics assumed for soil spring m.

Q and Ru. Q is the soil quake and represents the maximum deformation that may occur elastically. Ru is the ultimate ground resistance, or the load at which the soil spring behaves purely plastically.

A load-deformation diagram of the type shown in Figure 2 may be established separately for each spring. Thus, $K'(m)$ equals $Ru(m)$ divided by $Q(m)$, where $K'(m)$ is the spring constant (during elastic deformation) for external spring m.

Basic Equations—The following equations were developed by Smith (2):

$$D(m,t) = D(m,t-1) + 12\Delta t\, V(m,t-1) \tag{1}$$

$$C(m,t) = D(m,t) - D(m+1,t) \tag{2}$$

$$F(m,t) = C(m,t)K(m) \tag{3}$$

$$R(m,t) = [D(m,t) - D'(m,t)]\, K'(m)[1 + J(m)\, V(m,t-1)] \tag{4}$$

$$V(m,t) = V(m,t-1) + [F(m-1,t) - F(m,t) - R(m,t)]\frac{g\Delta t}{W(m)} \tag{5}$$

where

( ) = functional designation;
m = element number;
t = number of time interval;
Δt = size of time interval, sec;
$C(m,t)$ = compression of internal spring m in time interval t, in.;
$D(m,t)$ = displacement of element m in time interval t, in.;
$D'(m,t)$ = plastic displacement of external soil spring m in time interval t, in.;
$F(m,t)$ = force in internal spring m in time interval t, lb;
g = acceleration due to gravity, ft/sec^2;
$J(m)$ = damping constant of soil at element m, sec/ft;
$K(m)$ = spring constant associated with internal spring m, lb/in.;
$K'(m)$ = spring constant associated with external soil spring m, lb/in.;
$R(m,t)$ = force exerted by external spring m on element m in time interval t, lb;
$V(m,t)$ = velocity of element m in time interval t, ft/sec; and
$W(m)$ = weight of element m, lb.

This notation differs slightly from that used by Smith. Also, Smith restricts the soil damping constant J to 2 values, one for the point of the pile in bearing and one for the side of the pile in friction. Although the present knowledge of damping behavior of soils perhaps does not justify greater refinement, it is reasonable to use this notation as a function of m for the sake of generality.

The computations proceed as follows:

1. The initial velocity of the ram is determined from the properties of the pile driver. Other time-dependent quantities are initialized at zero or to satisfy static equilibrium conditions.
2. Displacements $D(m,1)$ are calculated by Eq. 1. It is to be noted that $V(1,0)$ is the initial velocity of the ram.
3. Compressions $C(m,1)$ are calculated by Eq. 2.
4. Internal spring forces $F(m,1)$ are calculated by Eq. 3.
5. External spring forces $R(m,1)$ are calculated by Eq. 4.
6. Velocities $V(m,1)$ are calculated by Eq. 5.
7. The cycle is repeated for successive time intervals.

Critical Time Interval

The accuracy of the discrete-element solution is also related to the size of the time increment Δt. Heising (4), in his discussion of the equation of motion for free longitudinal

vibrations in a continuous elastic bar, points out that the discrete-element solution is an exact solution of the partial differential equation when

$$\Delta t = \frac{\Delta L}{\sqrt{E/\rho}}$$

where ΔL is the segment length. Smith (3) draws a similar conclusion and has expressed the critical time interval as follows:

$$\Delta t = \frac{1}{19.648}\sqrt{\frac{W(m+1)}{K(m)}} \tag{6}$$

or

$$\Delta t = \frac{1}{19.648}\sqrt{\frac{W(m)}{K_m}} \tag{7}$$

If a time increment larger than that given by Eq. 6 is used, the discrete-element solution will diverge and no valid results can be obtained. As pointed out by Smith, in this case the numerical calculation of the discrete-element stress wave does not progress as rapidly as the actual stress wave. Consequently, the value of Δt given by Eq. 6 is called the "critical" value.

Effect of Gravity

The procedure as originally presented by Smith did not account for the static weight of the pile. In other words, at $t = 0$ all springs, both internal and external, exert zero force. Stated symbolically,

$$F(m,0) = R(m,0) = 0$$

If the effect of gravity is to be included, these forces must be given initial values to produce equilibrium of the system. A relatively simple scheme has been developed as a means of getting the gravity effect into the computations (27).

PILE-DRIVING HAMMERS

Energy Output of Impact Hammer

One of the most significant parameters involved in pile driving is the energy output of the hammer. This energy output must be known or assumed before the wave equation or dynamic formula can be applied. Although most manufacturers of pile driving equipment furnish maximum energy ratings for their hammers, these are usually downgraded by foundation experts for various reasons. A number of conditions such as poor hammer condition, lack of lubrication, and wear are known to seriously reduce energy output of a hammer. In addition, the energy output of many hammers can be controlled by regulating the steam pressure or quantity of diesel fuel supplied to the hammer. Therefore, a method was needed to determine a simple and uniform method that would accurately predict the energy output of a variety of hammers in general use.

Determination of Hammer Energy Output

Diesel Hammers—At present the manufacturers of diesel hammers arrive at the energy delivered per blow by 2 different methods. One manufacturer (5) feels that "Since the amount of (diesel) fuel injected per blow is constant, the compression pressure is constant, and the temperature constant, the energy delivered to the piling is also constant." The energy output per blow is thus computed as the kinetic energy of the falling ram plus the explosive energy found by thermodynamics. Other manufacturers

simply give the energy output per blow as the product of the weight of the ram-piston W_R and the length of the stroke h, or the equivalent stroke in the case of closed-end hammers.

The energy ratings given by these 2 methods differ considerably because the ram stroke h varies greatly. There is much controversy, therefore, as to which, if either, method is correct and what energy output should be used in dynamic pile analysis.

In conventional single-acting steam hammers, the steam pressure or energy is used to raise the ram for each blow. The magnitude of the steam force is too small to force the pile downward, and consequently it works only on the ram to restore its potential energy, $W_R \times h$, for the next blow. In a diesel hammer, on the other hand, the diesel explosive pressure used to raise the ram is, for a short time at least, relatively large (Fig. 3).

Although this explosive force works on the ram to restore its potential energy, $W_R \times h$, the initially large explosive pressure also does some useful work on the pile. Because the total energy output is the sum of the kinetic energy at impact plus the work done by the explosive force,

$$E_{total} = E_k + E_e \tag{8}$$

where

E_{total} = total energy output per blow;
E_k = kinetic energy of the ram at the instant of impact; and
E_e = the diesel explosive energy that does useful work on the pile.

It has been noted that, after the ram passes the exhaust ports, the energy required to comprss the air-fuel mixture is nearly identical to that gained by the remaining fall, d, of the ram (5). Therefore, the velocity of the ram at the exhaust ports is essentially the same as at impact, and the kinetic energy at impact can be closely approximated by

$$E_k = W_R(h - d) \tag{9}$$

where

W_R = ram weight;
h = total observed stroke of the ram; and
d = distance the ram moves after closing the exhaust ports and impacts with the anvil.

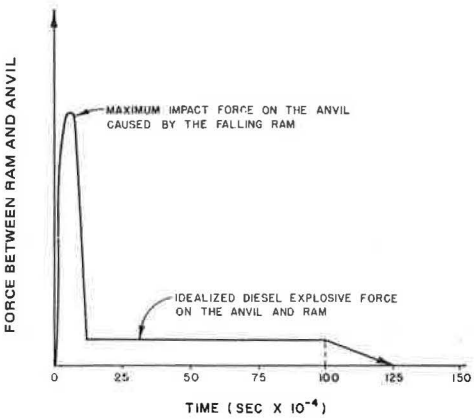

Figure 3. Typical force versus time curve for a diesel hammer.

The total amount of explosive energy $E_{e(total)}$ is dependent on the amount of diesel fuel injected, compression pressure, and temperature and, therefore, may vary somewhat.

Unfortunately, the wave equation must be used in each case to determine the exact magnitude of E_e because it depends not only on the hammer characteristics but also on the characteristics of the anvil, helmet, cushion, pile, and soil resistance. However, values of E_e determined by the wave equation for several typical pile problems indicate that it is usually small in proportion to the total explosive energy output per blow and, furthermore, that it is on the same order of magnitude as $W_R \times d$. Thus, assuming that

$$E_e = W_R \times d \tag{10}$$

and substituting Eqs. 9 and 10 into Eq. 8 give

$$E_{total} = E_k + E_e = W_R(h - d) + W_R d \tag{11}$$

so that

$$E_{total} = W_R h \tag{12}$$

The results given by this equation were compared with experimental values and the average efficiency was found to be 100 percent.

Steam Hammers—Using the same equation for comparison with experimental values indicated an efficiency rating of 60 percent for the single-acting steam hammers and 87 percent for the double-acting hammer, based on an energy output given by

$$E_{total} = W_R h \tag{13}$$

In order to determine an equivalent ram stroke for the double-acting hammers, the internal steam pressure above the ram that is forcing it down must be taken into consideration. The manufacturers of such hammers state that the maximum steam pressure or force should not exceed the weight of the housing or casing, or the housing may be lifted off the pile. Thus the maximum downward force on the ram is limited to the total weight of the ram and housing.

Because these forces both act on the ram as it falls through the actual ram stroke h, they add kinetic energy to the ram, which is given by

$$E_{total} = W_R h + F_R h \tag{14}$$

where

W_R = ram weight;
F_R = steam force not exceeding the weight of the hammer housing; and
h = observed or actual ram stroke.

Because the actual steam pressure is not always applied at the rated maximum, the actual steam force can be expressed as

$$F_R = \left(\frac{p}{P_{rated}}\right) W_H \tag{15}$$

where

W_H = hammer housing weight;
p = operating pressure; and
P_{rated} = maximum rated steam pressure.

The total energy output is then given by

$$E_{total} = W_R h + \left(\frac{p}{P_{rated}}\right) W_H h \tag{16}$$

This can be reduced in terms of Eq. 13 by using an equivalent stroke h_e that will give the same energy output as Eq. 16.

Thus,

$$E_{total} = W_R h_e \tag{17}$$

Setting Eqs. 16 and 17 equal yields

$$W_R h_e = W_R h + \left(\frac{p}{P_{rated}} W_H\right) h = h\left(W_R + \frac{p}{P_{rated}} W_H\right)$$

or solving for the equivalent stroke yields

$$h_e = h\left(1 + \frac{p}{P_{rated}} \times \frac{W_H}{W_R}\right) \tag{18}$$

Conclusions—The preceding discussion has shown that it is possible to determine reasonable values of hammer-energy output simply by taking the product of the ram weight and its observed or equivalent stroke and applying an efficiency factor. This method of energy rating can be applied to all types of impact pile drivers with reasonable accuracy.

Significance of Driving Accessories

In 1965 the Michigan Department of State Highways completed an extensive research program designed to obtain a better understanding of the complex problem of pile driving. Though a number of specific objectives were given, one was of primary importance. As noted by Housel (6), "Hammer energy actually delivered to the pile, as compared with the manufacturer's rated energy, was the focal point of a major portion of this investigation of pile-driving hammers." In other words, the researchers hoped to determine the energy delivered to the pile and to compare these values with the manufacturer's ratings.

The energy transmitted to the pile was termed ENTHRU by the investigators and was determined by the summation

$$\text{ENTHRU} = \Sigma F \Delta S$$

where F, the average force on the top of the pile during a short interval of time, was measured by a specially designed load cell, and ΔS, the incremental movement of the head of the pile during this time interval, was found by using displacement transducers or was reduced from accelerometer data or both. It should be pointed out that ENTHRU is not the total energy output of the hammer blow, but only a measure of that portion of the energy delivered below the load-cell assembly.

Many variables influence the value of ENTHRU. As was noted in the Michigan report: "Hammer type and operating conditions; pile type, mass, rigidity, and length; and the type and condition of cap blocks were all factors that affect ENTHRU, but when, how, and how much could not be ascertained with any degree of certainty." However, the wave equation can account for each of these factors so that their effects can be determined.

The maximum displacement of the head of the pile was also reported and was designated LIMSET. Oscillographic records of force versus time measured in the load cell were also reported. Because force was measured only at the load cell, the single maximum observed values for each case was called FMAX.

ENTHRU is greatly influenced by several parameters, especially the type, condition, and coefficient of restitution of the cushion, and the weight of extra driving caps.

The wave equation was therefore used to analyze certain Michigan problems to determine the influence of cushion stiffness, e, additional driving cap weights, and driving resistance encountered.

Table 1 gives data that show how ENTHRU and SET increase when the load cell assembly is removed from Michigan piles.

The data given in Table 2 show that ENTHRU does not always increase with increasing cushion stiffness. Furthermore, the maximum increase in ENTHRU noted here is relatively small—only about 10 percent.

TABLE 1

EFFECT OF REMOVING LOAD CELL ON ENTHRU, LIMSET, AND PERMANENT SET OF PILE

Case	Ram Velocity (ft/sec)	ENTHRU (kip/ft)		LIMSET (in.)		Permanent Set (in.)	
		With Load Cell	Without Load Cell	With Load Cell	Without Load Cell	With Load Cell	Without Load Cell
DTP-15, 80.5	8	1.5	1.6	0.27	0.34	0.23	0.25
	12	3.3	3.6	0.53	0.67	0.57	0.57
	16	5.8	6.5	1.02	1.03	0.94	0.97
	20	9.1	10.1	1.54	1.54	1.43	1.47
DLTP-8, 80.2	8	3.1	3.8	0.62	0.71	0.51	0.62
	12	7.1	8.5	1.15	1.32	1.06	1.29
	16	12.5	15.1	1.91	2.10	1.82	2.15
	20	19.5	23.6	2.70	3.08	2.65	3.13

TABLE 2

EFFECT OF CUSHION STIFFNESS ON ENERGY TRANSMITTED TO THE PILE (ENTHRU)

Ram Velocity (ft/sec)	RUT (kip)	ENTHRU (kip/ft) by Cushion Stiffness			
		540 kip/in.	1,080 kip/in.	2,700 kip/in.	27,000 kip/in.
8	30	3.0	3.0	3.0	2.9
	90	3.1	3.2	3.3	2.9
	150	3.0	3.2	3.3	3.0
12	30	6.6	6.4	7.1	6.4
	90	7.0	7.1	7.2	6.4
	150	6.9	7.2	7.4	6.7
16	30	11.8	11.9	12.2	11.3
	90	12.3	12.6	12.8	11.5
	150	12.4	12.9	13.2	11.4

When different cushions are used, the coefficient of restitution will probably change. Because the coefficient of restitution of the cushion may affect ENTHRU, a number of cases was solved with e ranging from 0.2 to 0.6. The data given in Tables 3 and 4 show that an increase in e from 0.2 to 0.6 normally increases ENTHRU from 18 to 20 percent, while increasing the permanent set from 6 to 11 percent. Thus, for the case shown, the coefficient of restitution of the cushion has a greater influence on rate of penetration and ENTHRU than does its stiffness. This same effect was noted in the other solutions, and results of the cases for which data are given in Tables 3 and 5 are typical of the results found in other cases.

The data given in Table 5 show that any increase in cushion stiffness also increases the driving stress. Thus, according to the wave equation, increasing the cushion stiffness to increase the rate of penetration (for example by not replacing the cushion until it has been beaten to a fraction of its original height or by omitting the cushion entirely) is both inefficient and poor practice because of the high stresses induced in the pile. It would be better to use a cushion having a high coefficient of restitution and a low cushion stiffness in order to increase ENTHRU and to limit the driving stress.

TABLE 3

EFFECT OF COEFFICIENT OF RESTITUTION ON MAXIMUM POINT DISPLACEMENT

Pile	RUT (kip)	Ram Velocity (ft/sec)	Maximum Point Displacement (in.)			Maximum Change (percent)
			e = 0.2	e = 0.4	e = 0.6	
BLTP-6, 10.0	30	12	2.13	2.14	2.36	10
		16	3.38	3.47	3.58	6
		20	4.73	4.93	5.17	8
BLTP-6, 57.9	150	12	0.46	0.48	0.50	8
		16	0.73	0.76	0.81	10
		20	1.05	1.10	1.18	11

TABLE 4

EFFECT OF COEFFICIENT OF RESTITUTION ON ENTHRU

Pile	RUT (kip)	Ram Velocity (ft/sec)	ENTHRU (kip/ft)			Maximum Change (percent)
			e = 0.2	e = 0.4	e = 0.6	
BLTP-6, 10.0	30	12	6.0	6.5	7.3	18
		16	10.5	11.8	12.8	18
		20	16.5	17.4	20.0	17
BLTP-6, 57.9	150	12	6.7	7.2	8.2	18
		16	11.6	12.7	14.5	20
		20	18.2	19.7	22.4	19

Unfortunately, the tremendous variety of driving accessories precludes general conclusions to be drawn from wave equation analyses in all but the most general of terms.

Although the effect of driving accessories is quite variable, it was generally noted that the inclusion of additional elements between the driving hammer and the pile or the inclusion of heavier driving accessories or both consistently decreased both the energy transmitted to the head of the pile and the permanent set per blow of the hammer. Increasing cushion stiffness will increase compressive and tensile stresses induced in a pile during driving. Table 6 gives data on the effect of cushion stiffness on the maximum displacement of the head of the pile.

CAP BLOCK AND CUSHIONS

Methods Used to Determine Cap Block and Cushion Properties

As used here, cap block refers to the material placed between the pile-driving hammer and the steel helmet, and cushion refers to the material placed between the steel helmet and pile (usually used only when concrete piles are driven). Although a cap block and cushion serve several purposes, their primary function is to limit impact stresses in both the pile and hammer. In general, it has been found that a wooden cap block is quite effective in reducing driving stresses, more so than a relatively stiff cap block material such as Micarta. However, the stiffer Micarta is usually more durable and transmits a greater percentage of the hammer's energy to the pile because of its higher coefficient of restitution.

For example, when 14 different cases in the Michigan study were solved by the wave equation, the Micarta assemblies averaged 14 percent more efficient than cap block assemblies of wood. However, the increased cushion stiffness in some of these cases increased the impact stresses. The increase in stress was particularly important when concrete or prestressed concrete piles were driven. When concrete piles are

TABLE 5

EFFECT OF CUSHION STIFFNESS ON MAXIMUM FORCE MEASURED AT THE LOAD CELL (FMAX)

Ram Velocity (ft/sec)	RUT (kip)	FMAX (kip) by Cushion Stiffness			
		540 kip/in.	1,080 kip/in.	2,700 kip/in.	27,000 kip/in.
8	30	132	185	261	779
	90	137	185	261	779
	150	143	186	261	779
12	30	198	278	391	1,169
	90	205	278	391	1,169
	150	215	279	391	1,169
16	30	264	371	522	1,558
	90	275	371	522	1,558
	150	288	371	522	1,558

TABLE 6

EFFECT OF CUSHION STIFFNESS ON MAXIMUM DISPLACEMENT OF THE HEAD OF THE PILE (LIMSET)

Ram Velocity (ft/sec)	RUT (kip)	LIMSET (in.) by Cushion Stiffness			
		540 kip/in.	1,080 kip/in.	2,700 kip/in.	27,000 kip/in.
8	30	1.09	1.08	1.08	1.13
	90	0.44	0.44	0.45	0.45
	150	0.32	0.33	0.33	0.33
	30	2.21	2.14	2.19	2.25
12	90	0.80	0.82	0.84	0.84
	150	0.55	0.57	0.58	0.58
	30	3.62	3.59	3.63	3.68
16	90	1.30	1.31	1.32	1.34
	150	0.85	0.87	0.88	0.90

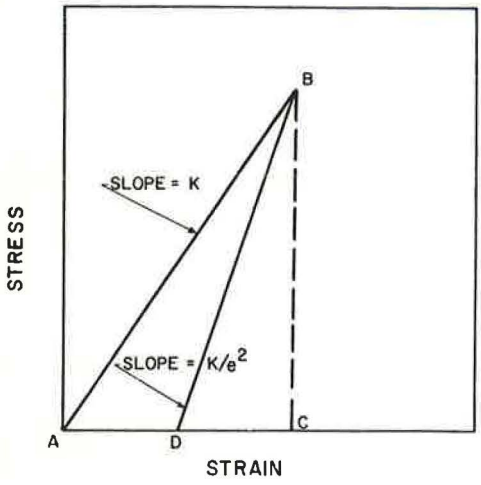

Figure 4. Stress-strain curve for a cushion block.

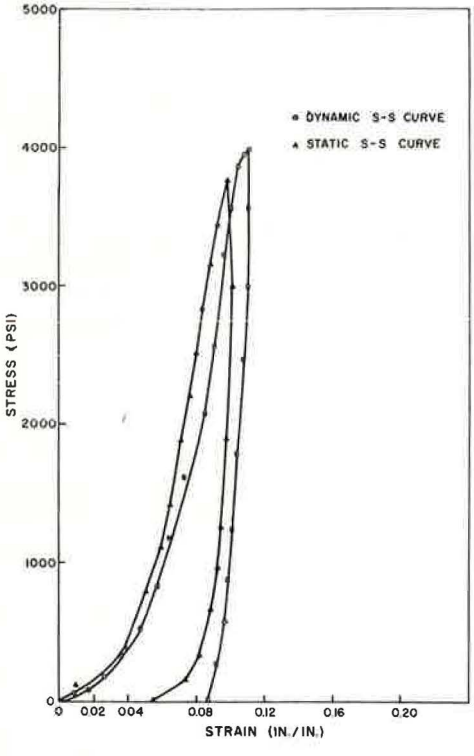

Figure 5. Dynamic and static stress-strain curves for a fir cushion.

TABLE 7

TYPICAL SECANT MODULI OF ELASTICITY E AND COEFFICIENTS OF RESTITUTION e OF VARIOUS PILE-CUSHIONING MATERIAL

Material	E (psi)	e
Micarta plastic	450,000	0.80
Oak (green)	45,000[a]	0.50
Asbestos disks	45,000	0.50
Fir plywood	35,000[a]	0.40
Pine plywood	25,000[a]	0.30
Gum	30,000[a]	0.25

[a]Properties of wood with load applied perpendicular to wood grain.

driven, it is also frequently necessary to include cushioning material between the helmet and the head of the pile to distribute the impact load uniformly over the surface of the pile head and prevent spalling.

To apply the wave equation to pile driving, Smith assumed that the cushion's stress-strain curve was a series of straight lines as shown in Figure 4.

Static and dynamic stress-strain properties were measured for several types of cushions. It was determined that the stress-strain curves were not linear as was assumed by Smith, but rather appeared as shown in Figure 5.

Surprisingly, the static and dynamic stress-strain curves for wooden cushions agreed remarkably well. A typical example of this agreement is shown in Figure 5. The stress-strain curves for a number of other materials commonly used as pile cushions and cap blocks, namely oak, Micarta, and asbestos, were also measured.

Idealized Load-Deformation Properties

The major difficulty encountered in trying to use the dynamic curves determined for the various cushion materials was that it was extremely difficult to input the information required by the wave equation. Although the initial portion of the curve was nearly parabolic, the top segment and unloading portion were extremely complex. This prevented the curve from being input in equation form and required numerous points on the curve to be specified.

Fortunately, it was found that the wave equation accurately predicted both the shape and the magnitude of the stress wave induced in the pile, even if a linear force-deformation curve was assumed for the cushion, so long as the loading portion was based on the secant modulus of elasticity for the material (as

opposed to the initial, final, or average modulus of elasticity) and the unloading portion was based on the actual dynamic coefficient of restitution. Typical secant moduli of elasticity values for various materials are given in Table 7.

Coefficient of Restitution

Although the cushion is needed to limit the driving stresses in both hammer and pile, its internal damping reduces the available driving energy transmitted to the head of the pile. Figure 4 shows this energy loss, with the input energy being given by the area ABC while the energy output is given by area BCD. This energy loss is commonly termed coefficient of restitution of the cushion e, in which

$$e = \sqrt{\frac{\text{area BCD}}{\text{area ABD}}}$$

Once the coefficient of restitution for the material is known, the slope of the unloading curve can be determined as shown in Figure 4.

For practical pile-driving problems, secant moduli of elasticity and coefficient of restitution values for well-consolidated cushions should be used. Table 7 also gives the coefficient of resitution for the materials that are recommended when the problem is analyzed by the wave equation.

SOIL PROPERTIES

A limited amount of work has been done on soil properties and their effects on the wave equation solution of the piling behavior problem (7, 8, 9). A brief summary of the results of these tests is given in this section.

Equations to Describe Soil Behavior

Examination of Eq. 19 show that Smith's equation describes a type of Kelvin rheological model as shown in Figure 6.

$$R(m,t) = [D(m,t) - D'(m,t)]\,K'(m)\,[1 + J(m)\,V(m,t-1)] \qquad (19)$$

The soil spring behaves elastically until the deformation D(m,t) equals Q, and then it yields plastically with a load-deformation property as shown in Figure 7a. The dashpot J develops a resisting force proportional to the velocity of loading V. Smith has

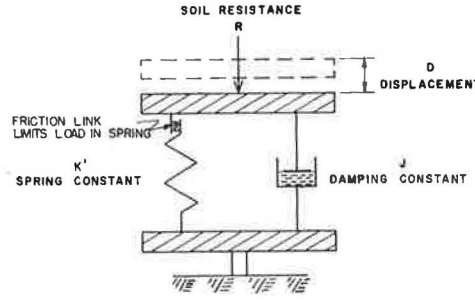

Figure 6. Model used by Smith to describe soil resistance on pile.

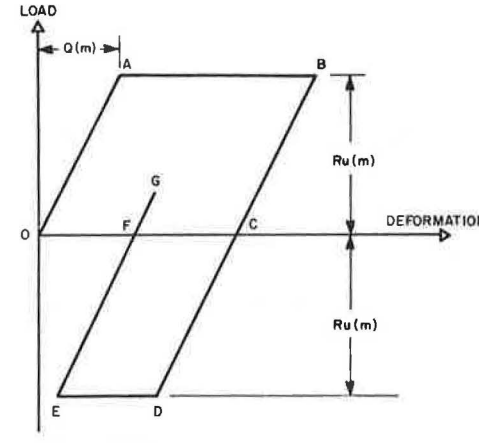

(a) STATIC

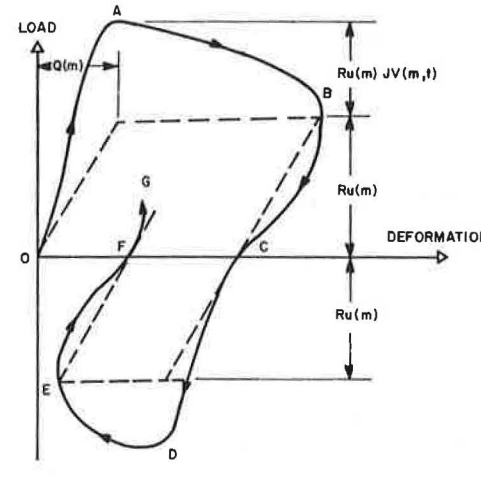

(b) DYNAMIC

Figure 7. Load-deformation characteristics of soil.

modified the true Kelvin model slightly as shown by Eq. 20. This equation will produce a dynamic load-deformation behavior shown by path OABCDEF in Figure 7b. If terms in Eq. 19 are examined, it can be seen that Smith's dashpot force is given by

$$[D(m,t) - D'(m,t)]K'(m)[J(m)\,V(m,t-1)] \tag{20}$$

The dimensions of J are sec/ft, and it is assumed to be independent of the total soil resistance or size of the pile. It is also assumed to be constant for a given soil under given conditions as is the static shear strength of the soil from which Ru on a pile segment is determined. Ru is defined as the maximum soil resistance on a pile segment.

Care must be used to satisfy conditions at the point of the pile. Consider Eq. 10 when m = p, where p is the number of the last element of the pile. K(p) is used as the point soil spring and J(p) as the point soil damping constant. Also at the point of the pile, the soil spring must be prevented from exerting tension on the pile point. The point soil resistance will follow the path OABCFG in Figure 7b. It should be kept in mind that at the pile point the soil is loaded in compression or bearing. The damping constant J(p) in bearing is believed to be larger than the damping constant J(m) in friction along the side of the pile.

Soil Parameters to Describe Dynamic Soil Resistance During Pile Driving

The soil parameters used to describe the soil resistance in the wave equation are Ru, Q, and J.

Soil resistance Ru—For the side or friction soil resistance, Ru is determined by the maximum static soil adhesion or friction against the side of a given pile segment by

$$Ru(m) = fs\,\Sigma_0\,\Delta L \tag{21}$$

where

fs = maximum soil adhesion or friction, lb/ft^2;
Σ_0 = perimeter of pile segment, ft; and
ΔL = length of pile segment, ft.

In cohesionless materials (sands and gravels)

$$fs = \bar{\sigma}\tan\phi' \tag{22}$$

where

$\bar{\sigma}$ = effective normal stress against the side of the pile, lb/ft^2; and
ϕ' = angle of friction between soil and pile, deg.

In cohesive soils (clays), fs during driving is the remolded adhesion strength between the soil and pile.

At the point of the pile, Ru is determined by the maximum static bearing strength of the soil and is found by

$$Ru = (Qu)(Ap) \tag{23}$$

where

Qu = ultimate bearing strength of soil, lb/ft^2; and
Ap = area of pile point, ft^2.

In cohesive soils (clays), it is believed that the undisturbed strength of the soil may be used conservatively to determine Qu, because the material at the pile point is in the process of being compacted and may even have a higher bearing value.

Quake Q—The value of Q, the elastic deformation of the soil, is difficult to determine for various types of soil conditions. Various sources of data indicate that values of Q in both friction and point bearing probably range from 0.05 to 0.15 in.

Chellis (10) indicates that the most typical value for average pile-driving conditions is Q = 0.10 in. If the soil strata immediately underlying the pile tip is very soft, it is possible for Q to go as high as 0.2 in. or more. At the present state of the art of pile-driving technology, it is recommended that a value of Q = 0.10 in. be used for computer simulation of friction and point soil resistance. However, in particular situations where more precise values of Q are known, they should be used.

Damping constant J—The Texas Transportation Institute has conducted static and dynamic tests on cohesionless soil samples to determine if Smith's rheological model adequately describes the load-deformation properties of these soils. Triaxial soil tests were conducted on Ottawa sand at different loading velocities. Figure 8 shows typical results from a series of such tests.

Figure 9 shows additional data concerning the increase in soil strength as the rate of loading is increased. Because these tests were confined compression tests, it is believed that they simulate to some extent the soil behavior at the pile point. The J-value increases as the sand density increases (void ratio e decreases), and it increases as the effective confining stress $\overline{\sigma}_3$ increases.

$$\overline{\sigma}_3 = \sigma_3 - u$$

where

σ_3 = total confining pressure; and
u = pore water pressure.

For saturated Ottawa sand specimens, J(p) varied from about 0.01 to 0.12. When the sand was dry J(p) was nominally equal to zero. These values of J(p) for sand are in reasonable agreement with those recommended by Smith (11) and Forehand and Reese (12)—0.1 to 0.4.

The value of J(p) for cohesive soils (clays) is not presently known. The very limited data available indicate it is at least equal to that for sand. Forehand and Reese believe it ranges from 0.5 to 1.0.

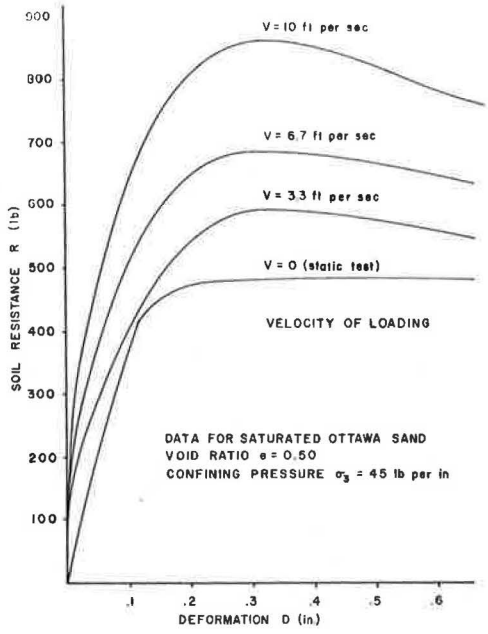

Figure 8. Load-deformation properties of Ottawa sand determined by triaxial tests (specimens 3 in. wide by 6.5 in. high).

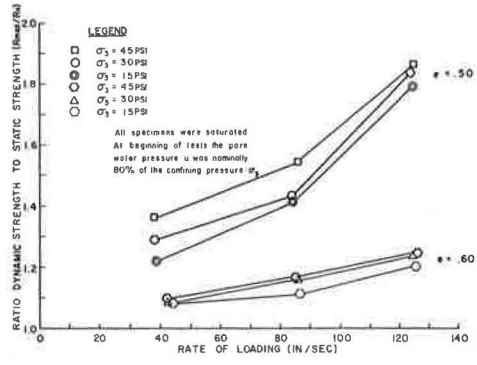

Figure 9. Increase in strength versus rate of loading for Ottawa sand.

There are no data now available to indicate the value of J(m) in friction along the side of the pile. Smith believes it is smaller than J(p) and recommends J(m) values in friction of about ⅓ those at the point. Research is under way at Texas A&M University that should indicate the value of J in friction. At the present time J(m) in friction or adhesion is assumed to be ⅓ of J(p).

Static Soil Resistance After Pile Driving (Time Effect)

Immediately after the pile is driven, the total static soil resistance or bearing capacity of the pile equals the sum of the Ru values discussed previously. Thus, Ru(total) is the bearing capacity immediately after driving.

$$Ru(total) = \sum_{m=1}^{m=p} Ru(m)$$

where

Ru(m) = soil adhesion or friction on segments m = 1 to m = p - 1, lb (note that this is the strength of the disturbed or remolded soil along the side of the pile); and

Ru(p) = bearing or compressive strength of soil at the pile point m = p, lb (note that this is taken as the strength of the soil in an undisturbed condition, which should be conservative).

As time elapses after the pile is driven, Ru(m) for m = 1 to p - 1 may increase as the disturbed or remolded soil along the side of the pile reconsolidates and the excess pore water pressure dissipates back to an equilibrium condition. In cohesive soils (clays) the increase in strength upon reconsolidation (sometimes referred to as setup) is often considerable.

The bearing capacity of the pile will increase as the remolded or disturbed clay along the side of the pile reconsolidates and gains strength, because the adhesion or friction strength of clay is generally restored with the passage of time. Loading tests at increasing intervals of time show that ultimate adhesion is approximately equal to the undisturbed cohesion. Therefore, the amount of increase in bearing capacity with time is related to the sensitivity and reconsolidation of the clay; sensitivity of clay = (undisturbed strength/remolded strength).

Figure 10 shows the time effect or setup of a pile driven in a cohesive soil. In cohesionless soils (sands and gravels) the friction strength of the soil will usually change very little. Normally, the value of Ru(p) at the pile point changes very little.

USE OF THE WAVE EQUATION TO PREDICT PILE LOAD-BEARING CAPACITY AT TIME OF DRIVING

In general, engineers are interested in the static load-carrying capacity of the driven pile. In the past the engineer has often had to rely on judgment based on simplified dynamic pile equations such as the Hiley or Engineering-News formulas. By the wave-equation method of analysis, a much more realistic engineering estimate can be made by using information generated by the program.

Previous sections have shown how the hammer-pile-soil system can be simulated and analyzed by the wave equation to determine the dynamic behavior of piling during driving. With this simulation, the driving stresses and penetration of the pile can be computed.

Wave Equation Method

In the field the pile penetration or permanent set per blow (in./blow) is observed, and this can be translated into the static soil resistance through the use of the wave equation.

Consider the example for soil that is a soft marine deposit of fine sand, silt, and muck, with the pile point founded on a dense layer of sand and gravel.

Steel step taper pile, ft	75
No. 00 Raymond hammer	
Efficiency, percent	80
Ram weight, lb	10,000
Energy, ft-lb	32,500
Micarta cap block	
K, lb/in.	6,600,000
e	0.8

Soil parameters assumed	
J(p) point, sec/ft	0.15
J(m) side, sec/ft	0.05
Q(p) point, in.	0.10
Q(m) side, in.	0.10
Soil distribution assumed	
Curve I	
Side friction (triangular distribution), percent	25
Point bearing, percent	75
Curve II	
Side friction (triangular distribution), percent	10
Point bearing, percent	90

Data shown in Figure 11 were developed by using J(point) = 0.3 for clay and J(point) = 0.1 for sand. The accuracy of the correlation, as shown in Figure 11, was approximately ±25 percent. Moseley (15) has found a similar correlation with 12 piles driven in sand. Figure 12 shows a summary of the data for the piles tested and shows that all resistances on these piles fall within ±20 percent of that predicted by the wave equation.

This information is used to simulate the system to be analyzed by the wave equation. A total soil resistance Ru(total) is assumed by the computer for analysis in the work. It then computes the pile penetration or permanent set when driven against this Ru(total). The reciprocal of permanent set is usually computed to convert this to blows per inch.

The computer program then selects a larger Ru(total) and computes the corresponding blows per inch. This is done several times until enough points are generated to develop a

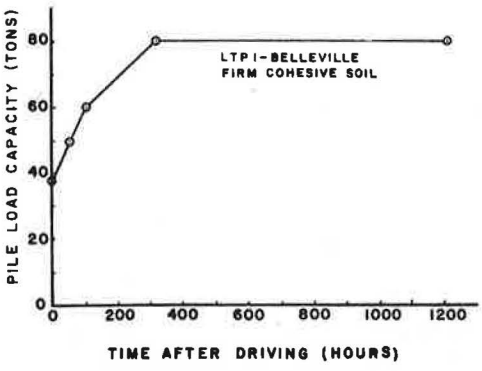

Figure 10. Setup or recovery of strength after driving in cohesive soil (13).

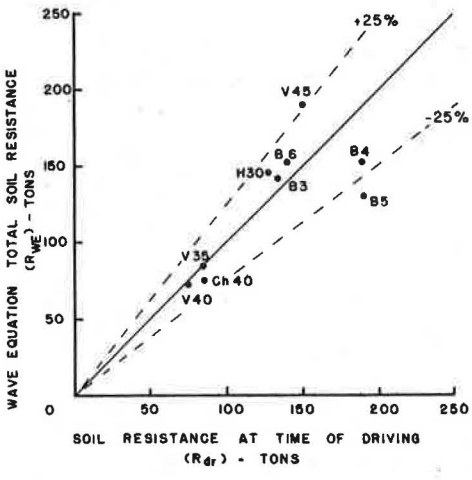

Figure 11. Comparison of wave-equation predicted soil resistance to soil resistance determined by load tests for piles driven in both sand and clay (14).

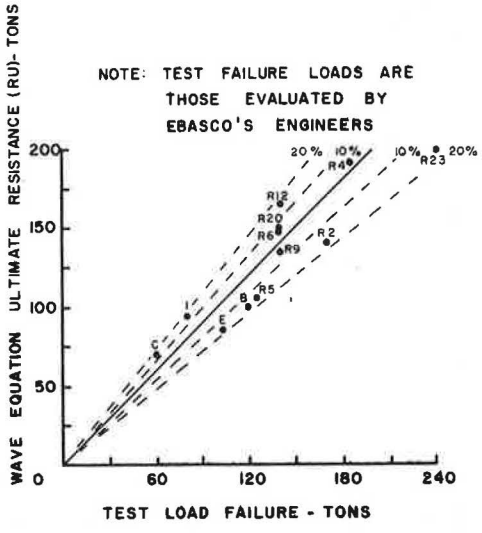

Figure 12. Wave-equation ultimate resistance versus test load failure (15).

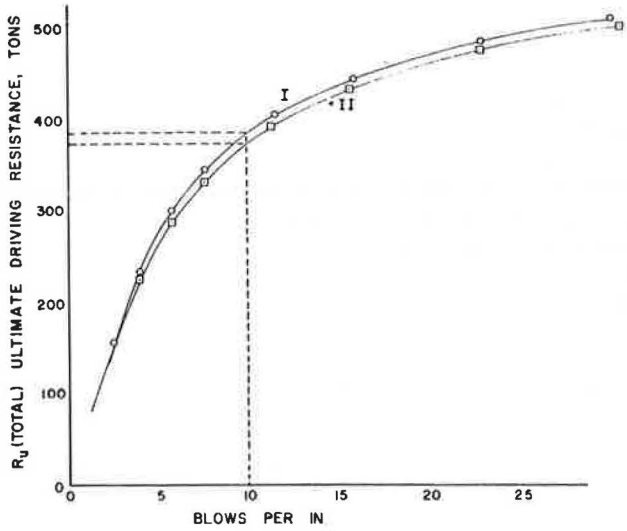

Figure 13. Ultimate driving resistance versus blows per inch for the example problem.

curve relating blows per inch to Ru(total) as shown in Figure 13 (2 curves for the 2 different assumed distributions of soil resistance are shown).

In the field if driving had ceased when the resistance to penetration was 10 blows/in. (a permanent set equal to 0.1 in./blow), then the ultimate pile load bearing capacity immediately after driving should have been approximately 370 to 380 tons as shown in Figure 13. It is again emphasized that this Ru(total) is the total static soil resistance encountered during driving, because the increased dynamic resistance was considered in the analysis by use of J. If the soil resistance is predominantly due to cohesionless materials such as sands and gravels, the time effect or soil setup that tends to increase the pile bearing capacity will be small or negligible. If the soil is a cohesive clay, the time effect or soil setup might increase the bearing capacity as discussed earlier. The magnitude of this setup can be estimated if the sensitivity and reconsolidation of the clay is known. It can also be conservatively disregarded because the setup bearing capacity is usually greater than that predicted by a curve similar to the one shown in Figure 13.

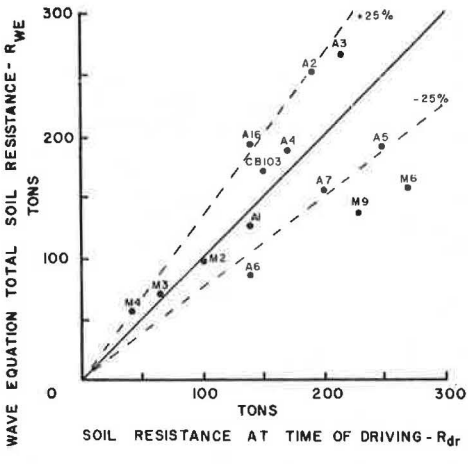

Figure 14. Comparison of wave-equation predicted soil resistance to soil resistance determined by load tests for piles driven in sands (14).

In developing the curves shown in Figure 13, it was necessary to assume that the soil parameters are distribution of soil resistance, soil quake Q, and soil damping constant J.

As shown by curves I and II in Figure 13, small variations in the distribution of soil resistance between side friction and point bearing will not affect the wave-equation results significantly. All that is required is a reasonable estimate of the situation. For

most conditions an assumption of soil quake Q = 0.1 in. is satisfactory. The value of J(m) is assumed to be ⅓ of J(p).

Comparison of Predictions With Field Tests

Correlations of wave-equation solutions with full-scale load tests to failure have provided a degree of confidence in the previously described method of predicting static bearing capacity.

For the sand-supported piles, damping constants of J(point) = 0.1 and J′(side) = J(point)/3 were found to give the best correlation. Figure 14 shows the accuracy of the correlation to be approximately ±25 percent.

For clay-supported piles, the damping constants J(point) = 0.3 and J′(side) = J(point)/3 gave the best correlation. The accuracy of the correlation is shown in Figure 15 to be approximately ±50 percent. If more than one soil was involved, the damping constant used was a weighted average.

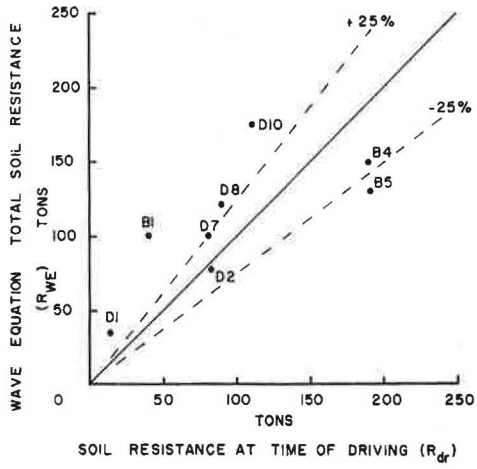

Figure 15. Comparison of wave-equation predicted soil resistance to soil resistance determined by load tests for piles driven in clay (14).

USE OF THE WAVE EQUATION FOR PARAMETER STUDIES

The wave equation can be used effectively to evaluate the effects of the numerous parameters that affect the behavior of a pile during driving. These include, for example, the determination of the optimum pile driver to drive a given pile to a specified soil resistance, the determination of the pile stiffness that will yield the most efficient use of a specified pile hammer and cushion assembly, the determination of the optimum cushion stiffness to make the most efficient utilization of a specified pile hammer and and driving assembly to drive a specific pile, and the determination of the effects of various distributions of soil side and point resistance on the pile bearing capacity, driving stresses, and penetration per blow.

Significant Parameters

The parameters that are known to significantly affect the behavior of a pile during driving are as follows:

1. The pile-driving hammer—(a) stiffness and weight of the pile-driver's ram; (b) energy of the falling ram that is dependent on the ram weight, the effective drop, and the mechanical efficiency of the hammer; (c) in the case of a diesel hammer, weight of the anvil and impulse of the explosive force; (d) stiffness of the cap block, which is dependent on its mechanical properties, thickness, cross-sectional area, and mechanical conditioning effects caused by repeated blows of the hammer; (e) weight of the pile helmet and the stiffness of the cushion between the helmet and the pile (in the case of steel piles the cushion is usually omitted); and (f) coefficient of restitution of the cap block and cushion that influences the shape of the wave induced in the pile and hence affects the magnitude of the stresses that are generated.
2. The pile—(a) length of the pile; (b) stiffness of the pile that is a function of its cross-sectional area and the modulus of elasticity of the pile material; (c) weight of the pile, specifically the distribution of the weight; and (d) existence of physical joints in the pile that cannot transmit tension.
3. The soil—(a) soil quake at the point; (b) soil quake in side friction; (c) damping constant of the soil at the point; (d) damping constant of the soil in friction; and (e) distribution of point and side frictional resistance.

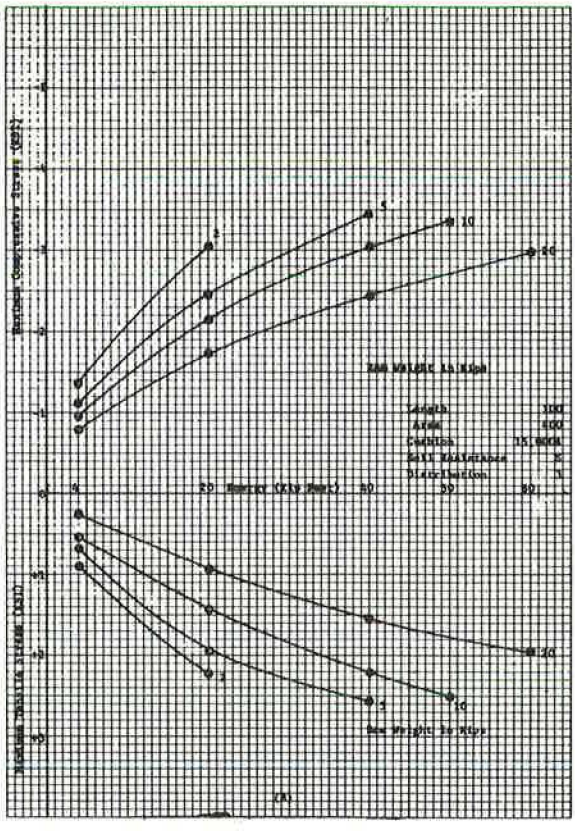

Figure 16. Effect of cushion stiffness, ram weight, and driving energy on stresses for square pile with uniformly distributed soil resistance of 107 tons.

Examples of Parameter Studies

The most notable parameter study that has been reported to date is that presented by Hirsch (16). In that report, the results of 2,106 problems are presented graphically. This study was oriented toward providing information on the effects of ram weight and energy, stiffness of cushion blocks, length of pile, soil resistance, and distribution of soil resistance on the driving behavior of representative square concrete piles. Figures 16 and 17 show representative curves from this study. The results of this study have played a very significant part in formulating recommended driving practices for prestressed concrete piles (17).

Parameter studies of this type have been used by others. McClelland, Focht, and Emrich (18) have used the wave equation to investigate the characteristics of available pile hammers for obtaining pile penetrations sufficient to support the heavy loads required in offshore construction. The parameters varied in this study were the pile length above the mud line, pile penetration, and the ratio of the soil resistance at the pile point to the total soil resistance (Fig. 18A). The results of this study enabled the authors to determine the pile-driving limit versus the design-load capacity as shown in Figure 19. Figure 18B shows the results of one study to determine the effects of varying the unembedded portion of a pile whose total length was held constant. Figure 18C shows the results for the same pile, but with the unembedded length held constant and the embedded length varied. Figure 18D shows the results when the ratio of point soil resistance to total resistance is varied.

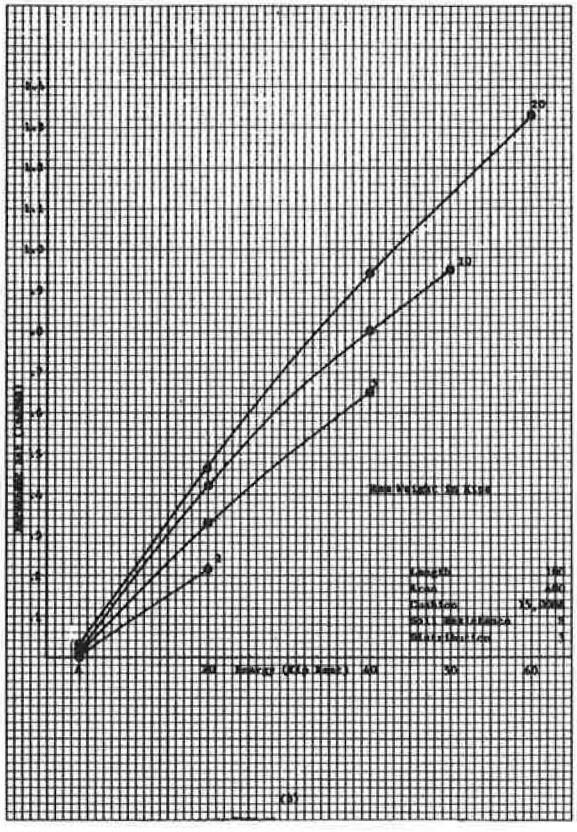

Figure 17. Effect of cushion stiffness, ram weight, and driving energy on permanent set for square pile with uniformly distributed soil resistance of 107 tons.

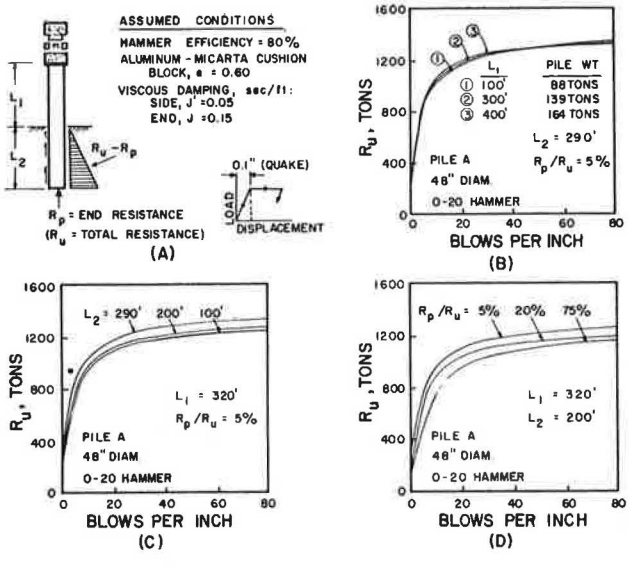

Figure 18. Computer analysis of pile-hammer effectiveness in overcoming soil resistance, Ru, when driving pile under varying conditions: (A) computer input representing conditions of problem; (B) variations in pile length above ground; (C) variations in pile penetration; (D) variations in distribution of soil resistance, Ru (18).

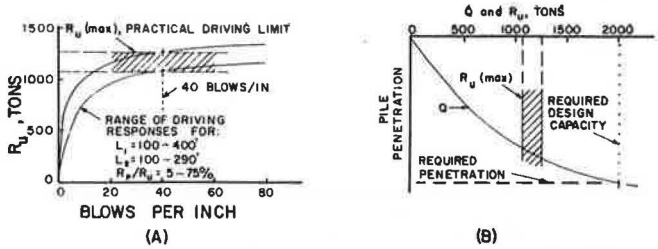

Figure 19. Evaluation of 0-20 hammer (60,000 ft-lb) for driving pile to develop ultimate capacity of 2,000 tons: (A) summary of wave equation analysis (Fig. 18) establishing approximate pile driving limit, Ru (max); (B) comparison of Ru (max) with required design capacity (18).

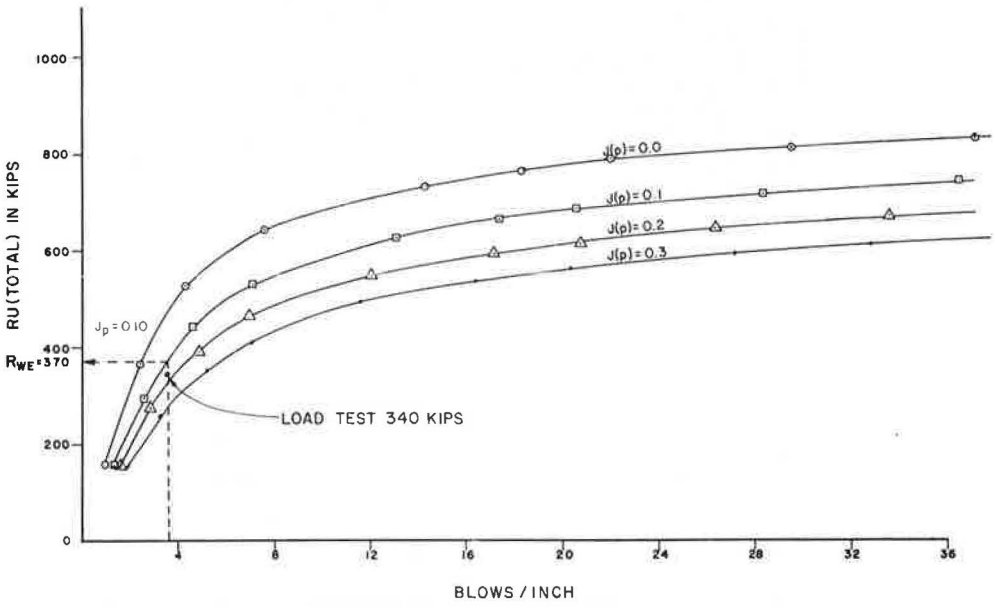

Figure 20. Blows/inch versus Ru (total) for Arkansas load test pile 4.

In an earlier report (14), the writers used the wave equation to determine the soil damping values for various soils encountered in field tests. In this particular parameter study, the pile-hammer-soil system was held constant and soil damping values were varied. By generating an ultimate soil resistance Ru(total) versus blows per inch curve, the appropriate soil damping properties could be determined by comparing the computer-generated solution with the measured data taken from a full-scale field test pile (Fig. 20). This study yielded representative values of the soil damping constants for the soil at the point of the pile and the soil in side friction.

It is not necessary that all parameters for a particular pile installation be known. For example, several problems can be solved in which the unknown parameter is varied between the upper and lower limits. These limits can usually be established with a reasonable amount of engineering judgment.

SUMMARY AND CONCLUSIONS

The numerical computer solution of the one-dimensional wave equation can be used with reasonable confidence for the analysis of pile-driving problems. The wave equation can be used to predict impact stresses in a pile during driving and can also be used to estimate the static soil resistance on a pile at the time of driving from driving records.

By using this method of analysis, the effects of significant parameters such as type and size of pile driving hammer, driving assemblies (cap block, helmet, and cushion block), type and size of pile, and soil condition can be evaluated during the foundation design stage. From such an analysis appropriate piles and driving equipment can be selected to correct or avoid expensive and time-consuming construction problems such as excessive driving stresses or pile breakage and inadequate equipment to achieve desired penetration or bearing capacity.

REFERENCES

1. Isaacs, D. V. Reinforced Concrete Pile Formula. Inst. Aust. Eng. Jour., Vol. 12, 1931.
2. Smith, E. A. L. Pile Driving Impact. Proc. Industrial Computation Seminar, Sept. 1950, International Business Machines Corp., New York, 1951.
3. Smith, E. A. L. Pile Driving Analysis by the Wave Equation. Proc. ASCE, Aug. 1960.
4. Heising, W. P. Discussion of Impact and Longitudinal Wave Transmission by E. A. L. Smith, Trans. ASME, Aug. 1955.
5. Rand, Mogens. Explosion Adds Driving Force to Diesel Hammer. Engineering Contract Record, Dec. 1960.
6. Housel, W. S. Pile Load Capacity: Estimates and Test Results. Jour. Soil Mechanics and Foundations Div., ASCE, Proc. Paper 4483, Sept. 1965.
7. Chan, P. C., Hirsch, T. J., and Coyle, H. M. A Laboratory Study of Dynamic Load-Deformation and Damping Properties of Sands Concerned With a Pile-Soil System. Texas Transportation Institute, Research Rept. 33-7, June 1967.
8. Reeves, G. N., Coyle, H. M., and Hirsch, T. J. Investigation of Sands Subjected to Dynamic Loading. Texas Transportation Institute, Research Rept. 33-7A, Dec. 1967.
9. Airhart, T. P., Hirsch, T. J., and Coyle, H. M. Pile-Soil System Response in Clay as a Function of Excess Pore Water Pressure and Other Soil Properties. Texas Transportation Institute, Research Rept. 33-8, Sept. 1967.
10. Chellis, R. D. Pile Foundations. McGraw-Hill, New York, 1951.
11. Smith, E. A. L. Pile Driving Analysis by the Wave Equation. Trans. ASCE, Vol. 127, Part I, Paper 3306, 1962.
12. Forehand, P. W., and Reese, J. L. Pile Driving Analysis Using the Wave Equation. Princeton Univ., MS in Eng. thesis, 1963.
13. Mansur, C. I. Pile Driving and Loading Test. Paper presented at ASCE Convention, New York, Oct. 22, 1964.
14. Lowery, L. L., Jr., Edwards, T. C., and Hirsch, T. J. Use of the Wave Equation to Predict Soil Resistance on a Pile During Driving. Texas Transportation Institute, Research Rept. 33-10, Aug. 1968.
15. Moseley, E. T. Test Piles in Sand at Helena, Arkansas: Wave Equation Analysis. Foundation Facts, Raymond International, Inc., New York, Vol. 3, No. 2, 1967.
16. Hirsch, T. J. A Report on Computer Study of Variables Which Affect the Behavior of Concrete Piles During Driving. Texas Transportation Institute, Aug. 1963.
17. Hirsch, T. J., and Samson, C. H. Driving Practices for Prestressed Concrete Piles. Texas Transportation Institute, Research Rept. 33-3, April 1965.
18. McClelland, B., Focht, J., and Emrich, W. Problems in Design and Installation of Heavily Loaded Pipe Piles. Paper presented at ASCE Specialty Conference on Civil Engineering in the Oceans, San Francisco, Sept. 1967.
19. Dunham, C. W. Foundations of Structures. McGraw-Hill, New York, 1962.
20. Fowler, J. W. Chesapeake Bay Bridge-Tunnel Project. Civil Engineering, Dec. 1963.

21. Leonards, G. A. Foundation Engineering. McGraw-Hill, New York, 1962.
22. Janes, R. L. Driving Stresses in Steel Bearing Piles. Illinois Institute of Technology, dissertation, June 1955.
23. Cummings, A. E. Dynamic Pile Driving Formulas. Jour. Boston Society of Civil Engineers, Jan. 1940.
24. Gardner, S. V., and Holt, D. Some Experiences With Prestressed Concrete Piles. Proc. Institute of Civil Engineers, London, Vol. 18, Jan. 1961.
25. Glanville, W. H., Grime, G., Fox, E. N., and Davies, W. W. An Investigation of the Stresses in Reinforced Concrete Piles During Driving. British Bldg. Research Board, Technical Paper 20, 1938.
26. Lowery, L. L., Hirsch, T. J., and Samson, C. H. Pile Driving Analysis—Simulation of Hammers, Cushions, Piles and Soils. Texas Transportation Institute, Research Rept. 33-9, Aug. 1967.
27. Samson, C. H., Hirsch, T. J., and Lowery, L. L. Computer Study of the Dynamic Behavior of Piling. Jour. Structural Div., Proc. ASCE, Paper 3608, Aug. 1963.
28. Hirsch, T. J. A Report on Stresses in Long Prestressed Concrete Piles During Driving. Texas Transportation Institute, Research Rept. 27, Sept. 1962.
29. Hirsch, T. J. A Report on Field Tests of Prestressed Concrete Piles During Driving. Texas Transportation Institute, Aug. 1963.
30. Hirsch, T. J., and Edwards, T. C. Impact Load-Deformation Properties of Pile Cushioning Materials. Texas Transportation Institute, Research Rept. 33-4, May 1966.